J. Phys. B: At. Mol. Opt. Phys. 21 (1988) 805-816. Printed in the UK

Continuum and bound states of the e^-–CH^+ system using the *R*-matrix method

Jonathan Tennyson

Department of Physics and Astronomy, University College London, Gower Street, London WC1E 6BT, UK

Received 21 September 1987, in final form 2 December 1987

Abstract. Molecular *R*-matrix calculations are performed on the astrophysically important e^--CH^+ system for internuclear separations in the range 1.5-4.0 a_0. The calculations are performed for both $^2\Pi$ and $^2\Sigma$ total symmetries. Several approximations, the most sophisticated being a polarised three-state close-coupling expansion, are employed. Many resonances below the CH^+ ($a\,^3\Pi$) threshold are resolved and classified using complex multichannel quantum defect theory. Scattering calculations with negative energy are used to obtain CH bound states. These yield a vertical ionisation energy in good agreement with experiment and estimates of the excitation energy to several excited states of $^2\Pi$ and $^2\Sigma$ symmetry, including some that have not previously been considered.

1. Introduction

CH^+ was the first interstellar molecular ion to be observed in the visible part of the spectrum. Its observed overabundance compared with theoretical predictions has long been an unresolved problem (Dalgarno 1976). Suggestions that CH^+ may be formed in interstellar shocks (Elitzer and Watson 1978, 1980) still lead to anomalies (Pineau des Forets *et al* 1986).

One means of removing CH^+ from the interstellar medium is via dissociative recombination:

$$CH^+ + e^- \rightarrow C + H. \tag{1}$$

The rate of this process was measured by Mui *et al* (1981), but there remain doubts about the vibrational distribution of the CH^+ in this experiment. Theoretically, attempts have been made to calculate dissociative recombination parameters (e.g. Raseev *et al* 1978, Giusti-Suzor 1979). However these calculations relied on relatively crude representation of the e^--CH^+ collision wavefunction. To date the most sophisticated e^--CH^+ scattering calculation appears to be that of Robb and Collins (1980), who performed static exchange calculations for a single CH^+ geometry.

Photoionisation of CH is also recognised as being an important astrophysical process. To be able to perform accurate *ab initio* photoionisation or dissociative recombination calculations it is necessary to have good e^--CH^+ continuum wavefunctions. This paper therefore reports results for the e^--CH^+ system at a range of internuclear separations using a method that has proved successful for the e^--H_2^+ system (Tennyson *et al* 1984, 1986, Tennyson and Noble 1985, Tennyson 1987). It is hoped that this work will form the first step in studying the processes discussed above. Results are reported for both bound and continuum states of the system calculated using the same methodology. Because of the relatively crude target wavefunction used

0953-4075/88/050805+12$02.50

in this work, the bound-state calculations cannot hope to replace highly correlated electronic structure calculations (e.g. Lie *et al* 1973, van Dishoeck 1987). Rather, they provide a method of assessing the accuracy of the scattering calculations. Thus, for example, quantum defect theory (Seaton 1983) suggests that the continuum will be well represented by a calculation which can reproduce the Rydberg series converging to the ground state of a target ion.

2. Method

The molecular R-matrix method has been developed by Burke, Noble and co-workers over a number of years; for a recent discussion of the theory see Gillan *et al* (1987). In the internal region, in these calculations a sphere of 10 a_0 centred at the CH^+ centre of mass, the wavefunction for the $(N+1)$-electron system can be written

$$\Psi_k = \mathscr{A} \sum_i a_{i,k} \Phi_i(x_1, \ldots, x_N) F_{i,k}(x_{N+1}) + \sum_j b_{j,k} \phi_j(x_1, \ldots, x_N, x_{N+1}). \tag{2}$$

The first sum in (2) runs over states of the N-electron target, characterised by Φ_i. The $(N+1)$-electron states are formed by antisymmetrising the product of the target states and continuum functions, $F_{i,k}$, of the appropriate symmetry. The continuum functions are expressed as a truncated partial wave expansion about the molecular centre of mass. The radial parts of the continuum functions are generated as numerical solutions of an isotropic model problem.

The continuum functions are of course not orthogonal to the target functions described above. This gave rise to considerable linear dependence problems in e^--CH^+ calculations with $^2\Sigma$ symmetry until a Lagrange orthogonalisation procedure (Tennyson *et al* 1987) was developed to cure this difficulty. In this procedure the σ-continuum functions are explicitly Lagrange orthogonalised to the three occupied target σ MO. The resulting reduced set of continuum orbitals is then Schmidt orthogonalised to the entire (occupied and virtual) set of target MO. For π-continuum orbitals simple Schmidt orthogonalisation to the target MO gave a well behaved orbital set.

The second sum in (2) runs over configurations composed entirely of L^2 orbitals. Such terms are included in the calculation to account for (*a*) high angular momentum effects in the region of the nuclei and (*b*) charge polarisation effects. These are included as one-particle-no-hole (1p, 0h) and two-particle-one-hole (2p, 1h) excitations of the target respectively.

The terms actually included in the two sums in (2) define the various models used to represent the scattering wavefunction in the internal region. The simplest model is the static exchange (SE) approximation in which the first sum in (2) is truncated at the ground state of the target and the second sum only includes (1p, 0h) configurations. Polarisation effects can be included either by including (2p, 1h) excitations (the SEP model) or by allowing for extra electronic states in the first sum. The use of excited electronic states in the close-coupling (CC) expansion has proved particularly important for resolving series of Feshbach resonances (Tennyson *et al* 1984, Tennyson and Noble 1985). This model will be referred to as the CCn approximation where n, here equal to 2 or 3, is the number of excited electronic states in the CC expansion. Finally it is possible to combine both methods of representing polarisation to give the close-coupling plus polarisation (CCnP) model. In this model only (2p, 1h) configurations from the target ground state are included.

Having solved the internal region problem (see Gillan *et al* 1987), it remains for the energy-dependent solutions to be found in the external region to yield the scattering parameters of the collision system. In the external region the wavefunction can be expanded as a single-centre, no-exchange solution of close-coupling equations. The direct potential, which can be written as a multipole expansion, provides the only off-diagonal coupling terms. In this work only the dipole and quadrupole moments of the CH^+ ground state along with the diagonal Coulombic term were retained in this potential expansion.

The solutions of the resulting close-coupled equations were found by propagating the R-matrix (Baluja *et al* 1982, Morgan 1984) to large r and then using the asymptotic code of Noble and Nesbet (1984). Bound states of the system were found by performing the scattering calculations at negative energy using the algorithm of Ohja and Burke (1983). Resonances were fitted to a Breit-Wigner form using an automatic detection and fitting procedure (Tennyson and Noble 1984). Because the $^1\Sigma^+$ and $^3\Pi$ states of CH^+ are close in energy (see below), it was necessary to propagate the coupled-state calculations to 100 and 150 a_0 using 35 R-matrix subranges to obtain converged results for bound and free scattering calculations respectively.

3. Calculations

In this work the CH^+ target was represented by a $12\sigma, 7\pi, 3\delta$ STO basis. The σ functions were those of Cade and Huo (1973). The higher symmetry orbitals were generated from the σ set by defining functions with $m = 1$ and $m = 2$ with the same exponent as the $m = 0$ orbitals and retaining all those with $l \geqslant m$.

The ground X $^1\Sigma^+$ state of CH^+ was represented by the SCF wavefunction. The lowest two excited states, a $^3\Pi$ and A $^1\Pi$, were obtained using one-particle excitation from the ground-state SCF 3σ orbital into the 1π orbital given by an SCF calculation on the a $^3\Pi$ state. Table 1 gives our result for the CH^+ target and compares with accurate calculations of Green *et al* (1971). It should be noted that our procedure gives X $^1\Sigma^+$ to a $^3\Pi$ excitation energies lower than those obtained from highly correlated

Table 1. Calculated energies of the lowest three states of CH^+ as a function of internuclear separation.

$R(a_0)$	1.5	1.8	2.0	2.137	2.3	2.5	3.0	4.0
$E(^1\Sigma^+)^a/E_h$	−37.793 91	−37.888 84	−37.907 26	−37.908 82	−37.903 47	−37.890 40	−37.845 42	−37.760 14
$E(^1\Sigma^+ \rightarrow {}^3\Pi)$ (eV)								
a	0.22	0.34	0.44	0.45	0.48	0.49	0.34	−0.32
b	0.31		0.63			0.88	0.99	0.46
c	1.01		1.13			1.43	0.94	0.43
$E(^1\Sigma^+ \rightarrow {}^1\Pi)$ (eV)								
a	3.98	3.73	3.52	3.34	3.12	2.83	2.10	1.01
b	3.28		3.29			3.06	2.26	0.79
c	3.55		3.29			2.77	2.13	0.86

[a] This work.
[b] Green *et al* (1971), (MC)SCF calculation.
[c] Green *et al* (1971), SCF-CI calculation.

structure calculations. Indeed, at the largest internuclear separation considered, $R = 4.0\ a_0$, the two states were found to cross instead of going smoothly to the same dissociation limit. Conversely the $X\ ^1\Sigma^+$ to $A\ ^1\Pi$ excitation energy is well represented by this procedure. This problem is associated with the SCF approximation as the correlation energy of the singlet states is larger than that of the $a\ ^3\Pi$ state. Green *et al* (1971) only partially solved this problem by using a two-state MCSCF calculation to represent the CH^+ ground state.

Continuum functions with $l \leqslant 6$ were included in the basis. The radial part of the continuum basis functions were generated as all the numerical solutions with $k^2 \leqslant 9$ Ryd of a simple Coulomb potential with $Z = 1$ inside the R-matrix sphere. This gave about eight numerical functions per channel.

Table 2 reports eigenphase sums for scattering calculations performed within the SE and SEP approximations. The SE results agree with the results of Robb and Collins (1980) to approximately within their claimed 10% accuracy limit. The sensitivity of the $^2\Sigma$ eigenphase to the addition of extra σ correlation functions suggests that functions with high l are important in the region of the nuclear singularities for the penetrating $^2\Sigma$ symmetry.

Table 2. Eigenphase sums for low-energy, elastic e^--CH^+ scattering for $R = 2.137\ a_0$.

	$^2\Sigma$		$^2\Pi$	
k^2(Ryd)	0.01	0.05	0.01	0.05
SE				
2 corr[a]	−0.562	−0.556	−1.306	−1.307
3 corr[a]	−0.413	−0.403	−1.305	−1.306
b	−0.612	−0.568	−1.286	−1.287
SEP				
2 corr[a]	−0.188	−0.177	−0.909	−0.796
3 corr[a]	0.048	0.054	−0.850	−0.678

[a] Number of $\sigma(\pi)$ symmetry virtual orbitals available in the $^2\Sigma(^2\Pi)$ symmetry calculation.
[b] Robb and Collins (1980).

The SEP results show that polarisation effects cause large changes in the eigenphases. At this level of approximation, one finds resonances which correspond to doubly excited states of CH. As will be shown below, this resonance structure is very dense in the low-energy scattering region. Furthermore, the inclusion of polarisation gives a more attractive potential which causes a resultant increase in the background eigenphase.

Successive calculations which increased the number of virtual orbitals available for building the polarisation potential showed that the positions of the resonances were far from being converged at this level of approximation. This observation is in line with previous experience (Schneider and Collins 1983, Tennyson *et al* 1984, Tennyson and Noble 1986) which has shown that this method of stabilising Feshbach resonances is only slowly convergent. It was therefore decided to perform calculations which explicitly included the low-lying electronically excited states of CH^+ in the close-coupling expansion.

Besides the $X\ ^1\Sigma^+$ ground state, CH^+ has one very low-lying electronic state, with $^3\Pi$ symmetry, and a low-lying $^1\Pi$ state. These are the states detailed in table 1. All

the other electronically excited states of CH^+ lie entirely above its dissociation limit. Two- and three-coupled-state calculations were performed with these states. The calculations with $^2\Pi$ total symmetry only allowed for coupling to continuum functions of σ and π symmetry. One would expect the δ-symmetry continuum to be less important (Tennyson and Noble 1986), but its neglect means that series of resonances corresponding to these partial waves have not been allowed for in the calculations. The following section gives the results of the coupled-state calculations.

4. Results

4.1. Bound states of CH

In this section results are presented for bound states of CH with $^2\Sigma$ and $^2\Pi$ symmetry. The bound-state calculations were performed not to supersede the accurate electronic structure calculations and experiments that are available for this system, but to try and gauge the accuracy of the calculations before embarking on a study of the continuum states of the system for which there are few data to compare with.

During the course of this work van Dishoeck (1987) reported a comprehensive study of CH bound states. Table 3 compares the present CH with the calculations of van Dishoeck (1987), Lie *et al* (1973) and the experiments of Herzberg and Johns (1969). It should be noted that our calculations are for the CH^+ equilibrium separation of 2.137 a_0 as against the CH equilibrium value of 2.116 a_0 used in the other calculated transition energies and the experimental (0, 0) band energies.

Table 3. Vertical electronic excitation energies and ionisation potential, in eV, for the X $^2\Pi$ state of CH at its equilibrium geometry.

Model	Ionisation potential	C $^2\Sigma$	$2^2\Sigma$	$3^2\Sigma$	$2^2\Pi$	$3^2\Pi$	$4^2\Pi$
CC2	9.88	4.22	6.15	7.67	6.95	7.61	8.47
CC2P	10.82	4.55	6.85	8.53	7.80	8.46	9.29
CC3	10.03	4.12	6.03	7.78	7.10	7.72	8.57
CC3P	10.83	4.53	6.76	8.51	7.81	8.45	9.29
a		4.02	6.39	7.96	7.43	7.94	8.05
b		4.02					
c	10.64	3.98		8.00	7.31	7.96[d]	

[a] Calculated (van Dishoeck 1987).
[b] Calculated (Lie *et al* 1973).
[c] Observed (Herzberg and Johns 1969).
[d] Assignment uncertain.

Our calculations show little sensitivity to the inclusion of the A $^1\Pi$ state in the close-coupling expansion, but significant differences when (2p, 1h) configurations were included in the wavefunction. These configurations were generated by allowing all (2p, 1h) excitations from the $1\sigma^2$, $2\sigma^2$, $3\sigma^2$ orbitals into 4σ, 5σ, 6σ, 1π, 2π, 3π, 1δ, 2δ virtual orbitals.

The most sophisticated calculation, CC3P, gives an ionisation potential within 2% of the experimental value. This agreement is impressive and probably not fortuitous as previous R-matrix calculations have been able to reproduce relative positions for

curves of N- and $(N+1)$-electron systems (Morgan and Noble 1984, Morgan and Burke 1988). Conversely the excitation energies appear to be given better by the CC2 and CC3 calculations. It would appear that the short-range polarisation expansion preferentially correlates the CH ground state relative to the excited states which leads to an almost uniform increase of about 0.5 eV in the transition energies on going from the CCn to the CCnP calculations.

Figure 1 presents results for the lowest six $^2\Sigma$ and $^2\Pi$ symmetry states of CH as a function of internuclear separation. These curves show structure due to avoided crossings, all of which can also be found in the results of van Dishoeck (1987). Figure 1 includes curves for several states not considered in table 3. To our knowledge these are the first predictions of any sort for these high-lying states.

4.2. Elastic scattering below the $^3\Pi$ threshold

Table 4 gives positions and widths for the lowest 11 (12) resonances lying 0.05 Ryd above threshold and below the CH^+ (a $^3\Pi$) threshold, as functions of the approximation.

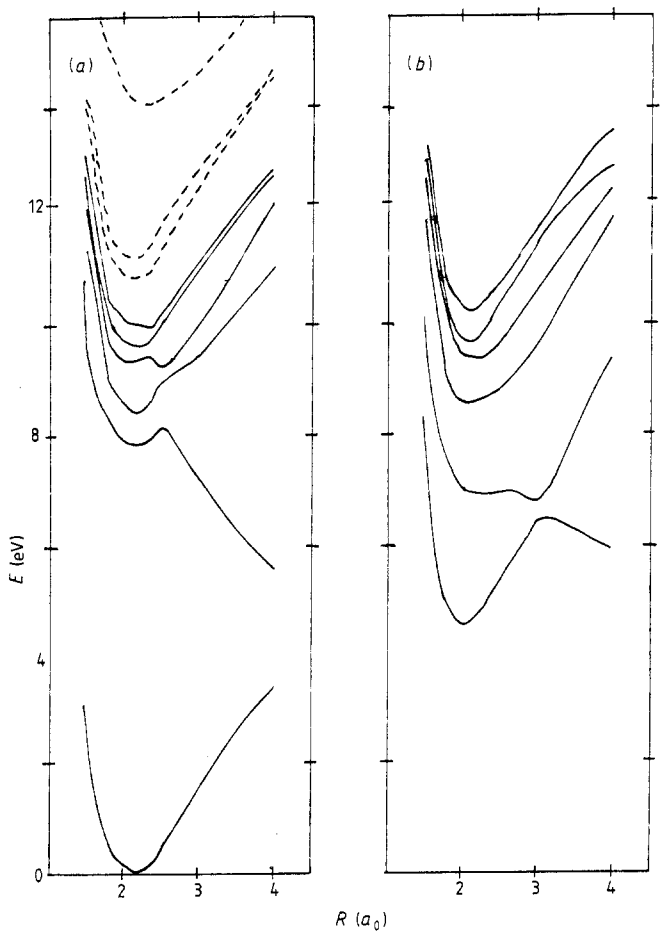

Figure 1. Potential energy curves for the six lowest states of CH with (*a*) $^2\Pi$ and (*b*) $^2\Sigma$ symmetry. The broken curves represent the three lowest states of CH^+.

Table 4. Resonance parameters, in Ryd, for the lowest resonances in coupled-state e^--CH^+ scattering calculations with $^2\Sigma$ symmetry. The CH^+ is fixed at $R = 2.137\ a_0$. (Powers of ten given in parentheses).

CC2		CC2P		CC3P	
E	Γ	E	Γ	E	Γ
				0.005 14	3.9 (−6)
0.005 23	8.0 (−7)	0.005 22	1.4 (−6)	0.005 25	1.1 (−6)
0.005 58	6.1 (−6)	0.005 49	8.7 (−6)	0.005 48	2.3 (−5)
0.010 37	3.3 (−5)	0.010 11	1.5 (−5)	0.009 03	4.5 (−4)
0.012 41	4.3 (−6)	0.012 36	1.1 (−5)	0.011 52	1.6 (−4)
0.012 59	6.5 (−7)	0.012 58	1.1 (−6)	0.012 52	2.5 (−6)
0.012 81	3.8 (−6)	0.012 75	5.4 (−6)	0.012 75	1.4 (−5)
0.015 90	2.2 (−5)	0.015 73	9.3 (−6)	0.015 01	3.0 (−4)
0.017 24	2.9 (−6)	0.017 22	7.1 (−6)	0.016 63	1.1 (−4)
0.017 37	5.0 (−7)	0.017 37	8.6 (−7)	0.017 32	1.6 (−6)
0.017 52	2.6 (−6)	0.017 48	3.6 (−6)	0.017 48	9.4 (−6)
0.019 62	1.5 (−5)	0.019 50	6.4 (−6)	0.019 01	2.0 (−4)

The positions of the resonances are not greatly affected by the inclusion of short-range polarisation in the calculation, but appear sensitive to addition of the third state to the close-coupling expansion. This behaviour is the converse of that shown by the bound states in table 3 which is probably a reflection of the more diffuse nature of the resonance rather than truly bound states of the system. The resonance widths, however, appear sensitive to all improvements of the wavefunction, showing a general increase by an order of magnitude between the CC2 and CC3P calculations.

The large number of resonances displayed in the small energy region covered by table 4 is a reflection of the closeness of the $^3\Pi$ threshold. It would be nice to assign these resonances to specific continuum states of the system, but their narrowness makes this difficult by methods such as inspection of eigenphase sums. This situation is further complicated when the calculations are repeated as a function of CH^+ internuclear separation. In this case one would like to match resonances between neighbouring geometries and hence draw families of resonance curves. These curves, and in particular where they become bound states, have an important role to play in the dissociative recombination process. However, the sheer density of resonances makes any matching by simple energy (and width) comparisons impossible. For this reason it was decided to analyse the results using quantum defect theory (Seaton 1983, Moores and Saraph 1983). As we shall see, this theory also has the advantage that information can be obtained about resonances missed in the automatic fitting procedure.

Tables 5 and 6 present complex quantum defect parameters (Seaton 1969, Norcross and Seaton 1970) for the resonances found at least 0.05 Ryd below the $^3\Pi$ threshold, E_{thresh}, as a function of CH^+ internuclear separation using a mesh spacing of 3×10^{-5} Ryd. For each resonance the quantities tabulated are the effective quantum number of the resonance, ν, and twice the complex quantum defect, 2β. These were obtained from the fitted position, E_{res}, and width, Γ, using the formulae

$$E_{\text{res}} = E_{\text{thresh}} - \frac{1}{\nu^2} \qquad \Gamma = \frac{2\beta}{\nu^3} \tag{3}$$

where the energies are in Ryd and other quantities in atomic units.

Table 5. Quantum defect parameters, $(\nu, 2\beta)$, for the low-lying resonances in e^--CH^+ with $^2\Sigma$ symmetry. (Powers of ten given in parentheses.)

R 1.5	1.8	2.0	2.137	2.3	2.5	3.0
				5.952 5.2 (−3)	5.934 1.1 (−2)	
			6.001 3.0 (−4)	6.001 3.2 (−4)	6.001 3.5 (−4)	
			6.031 1.8 (−3)	6.036 2.1 (−3)	6.043 2.3 (−3)	
		6.597 1.6 (−2)	6.591 2.7 (−3)	6.585 1.8 (−3)	6.551 4.0 (−3)	
		6.980 2.8 (−3)	6.964 3.5 (−3)	6.951 4.0 (−3)	6.933 6.3 (−3)	
		7.008 3.4 (−4)	7.002 3.7 (−4)	7.002 4.2 (−4)		
		7.045 1.7 (−2)	7.031 1.8 (−3)	7.036 2.0 (−3)	7.044 2.3 (−3)	
	7.591 4.7 (−3)	7.599 3.7 (−3)	7.601 3.3 (−2)	7.580 1.8 (−3)	7.520 1.3 (−2)	7.663 6.2 (−3)
	7.986 1.7 (−3)	7.983 2.9 (−3)	7.964 3.5 (−3)	7.951 9.1 (−3)	7.933 7.8 (−2)	7.900 4.0 (−3)
			8.002 4.3 (−4)	8.002 4.5 (−4)	8.002 4.8 (−4)	8.003 1.1 (−6)
		8.036 1.6 (−3)	8.031 1.8 (−3)	8.037 2.0 (−3)	8.044 2.3 (−3)	8.065 3.0 (−3)
	8.590 4.6 (−3)	8.602 3.6 (−3)	8.588 2.4 (−3)	8.576 1.9 (−3)	8.484 2.7 (−2)	8.660 5.7 (−3)
	8.986 1.7 (−3)	8.987 2.9 (−3)	8.964 3.6 (−3)	8.950 4.1 (−3)	8.931 5.3 (−3)	8.899 4.0 (−3)
				9.002 5.0 (−4)		9.003 5.6 (−4)
		9.040 1.4 (−3)	9.031 1.8 (−3)	9.037 2.0 (−3)	9.044 2.4 (−3)	9.065 3.0 (−3)
9.585 4.6 (−3)	9.590 4.6 (−3)	9.606 3.5 (−3)	9.587 2.4 (−3)	9.572 2.0 (−3)		9.658 5.4 (−3)
	9.986 1.7 (−3)	9.991 2.9 (−3)	9.957 0.208	9.950 4.1 (−3)		9.899 4.0 (−3)
10.019 1.1 (−3)		10.045 1.6 (−3)	10.031 1.8 (−3)			10.065 3.0 (−3)
10.585 4.6 (−3)	10.590 4.6 (−3)	10.611 3.5 (−3)	10.586 2.3 (−3)			10.656 5.2 (−3)
	10.986 1.7 (−3)	10.997 2.9 (−3)	10.963 3.6 (−3)			10.898 4.0 (−3)
11.004 7.0 (−5)	11.002 3.7 (−4)					11.003 6.9 (−4)
11.585 4.6 (−3)	11.590 4.5 (−3)	11.618 3.4 (−3)				11.655 5.1 (−3)
	11.986 1.7 (−3)					11.898 4.0 (−3)

The real part of the quantum defect, α, for a particular level is then given by

$$\nu = n - \alpha \tag{4}$$

where n is an integer and the complex quantum defect, μ, is given by

$$\mu = \alpha + i\beta \tag{5}$$

where α and β are assumed to vary smoothly and usually slowly with n.

Inspection of tables 5 and 6 shows that all the resonances represented appear to be part of series converging to the $^3\Pi$ threshold. No evidence could be found for any resonances associated with the $^1\Pi$ state, although the $R = 2.5$ $^2\Pi$ symmetry parameters do appear less regular due to some perturbation. As σ- and π-continuum functions with $l \leqslant 6$ were included the basis, one would expect six series of resonances for each geometry for $^2\Sigma$ symmetry and seven for $^2\Pi$ symmetry. Inspection of the tables shows that not all these series are resolved. Furthermore, not all members of the series that were detected are present. This is not caused by the narrowness of the resonances, but their density.

As there are several resonances clustered about $\nu \simeq n$ ($\alpha \simeq 0$), it proved difficult to resolve all of these, the tendency being only for the broadest to be detected. For example, for the $^2\Pi$ symmetry with $R = 2.137$ a_0, only one member of the series with $\alpha = -0.005$ has been resolved. Inspection of the eigenphase sums at $k^2 = 0.012\,60$ Ryd, where one would expect the $n = 7$ member of the series, shows that there is indeed a resonance but that the resonance was too close to the resonance at 0.012 52 Ryd ($\nu = 6.990$). These resonances have widths 7×10^{-7} and 2×10^{-6}, and therefore do not overlap. The problem is thus one of not having sufficient mesh points between the two for detection of both.

Table 6. Quantum defect parameters, $(\nu, 2\beta)$, for the low-lying resonances in e^--CH^+ with $^2\Pi$ symmetry. (Powers of ten given in parentheses.)

R 1.5	1.8	2.0	2.137	2.3	2.5	3.0
				5.740 7.3 (−2)		
			5.992 8.4 (−4)	5.985 1.2 (−3)	5.965 5.8 (−3)	
			6.005 2.5 (−4)		6.004 5.8 (−4)	
			6.030 5.0 (−3)	6.035 3.1 (−3)	6.043 1.9 (−3)	
		6.461 0.110	6.462 0.122	6.449 0.169	6.159 0.142	
		6.883 3.5 (−2)	6.825 5.1 (−2)	6.718 6.3 (−2)	6.553 1.2 (−2)	
			6.990 8.4 (−4)	6.983 1.1 (−3)	6.949 2.6 (−2)	
		7.000 6.5 (−4)			7.003 3.6 (−3)	
		7.034 7.6 (−3)	7.030 4.9 (−3)	7.035 3.1 (−3)	7.043 3.2 (−3)	
	7.440 8.5 (−2)	7.464 0.107	7.460 0.123	7.435 0.183		7.555 0.152
	7.924 2.2 (−2)	7.882 3.8 (−2)	7.819 5.0 (−2)	7.701 5.3 (−2)	7.547 2.2 (−2)	7.612 7.2 (−2)
			7.989 8.3 (−4)	7.982 9.7 (−4)	7.921 7.8 (−2)	7.956 1.4 (−2)
		8.002 7.7 (−4)			8.002 6.2 (−2)	
	8.026 1.5 (−2)				8.016 2.1 (−2)	8.011 2.1 (−3)
		8.038 7.4 (−3)	8.031 4.9 (−3)	8.036 3.2 (−3)	8.047 4.0 (−2)	8.072 3.1 (−4)
	8.444 8.6 (−2)	8.468 0.106	8.459 0.124	8.419 0.195		8.550 0.164
	8.923 2.0 (−2)	8.884 3.4 (−2)	8.815 5.0 (−2)	8.687 4.4 (−2)	8.545 2.8 (−2)	8.605 4.8 (−2)
			8.989 8.1 (−4)	8.981 9.1 (−4)	8.890 0.111	8.954 1.4 (−2)
		9.006 6.9 (−4)			9.013 9.8 (−3)	9.012 2.0 (−3)
	9.026 1.3 (−2)	9.042 7.3 (−3)	9.031 4.8 (−3)	9.036 3.2 (−3)		
9.440 8.5 (−2)	9.445 8.6 (−2)	9.472 0.106	9.457 0.125	9.402 0.206		9.546 0.171
9.963 7.6 (−3)	9.922 1.9 (−2)	9.888 3.4 (−2)	9.812 4.9 (−2)	9.676 3.6 (−2)	9.543 3.3 (−2)	9.605 4.7 (−2)
			9.988 6.7 (−4)	9.980 8.7 (−4)		9.54 1.2 (−2)
10.030 1.3 (−2)	10.027 1.3 (−2)	10.046 7.1 (−3)		10.036 3.2 (−3)		
10.441 8.6 (−2)	10.446 8.6 (−2)	10.478 0.106				
10.963 7.7 (−3)	10.921 1.9 (−2)	10.893 3.4 (−2)				10.604 4.1 (−2)
						10.952 1.2 (−2)
11.030 1.2 (−2)	11.027 1.3 (−2)					
11.443 8.6 (−2)	11.447 8.5 (−2)					
11.963 7.4 (−3)	11.921 1.9 (−2)					11.603 3.9 (−2)
						11.952 1.0 (−2)

The complex quantum defects given in tables 5 and 6 are no more than a convenient parametric representation of the fitted resonance position and widths. However it is possible to obtain direct information about the quantum defects by extrapolating through threshold (Seaton 1983). One can then analyse the eigenvalues of the portion of the S matrix, χ_{cc}, pertaining to the newly opened channels. Tables 7 and 8 present the results of analysing scattering calculations performed 0.05 Ryd above E_{thresh}. One advantage of this method of generating the quantum defects is that the eigenvectors of the K matrix can be used to make assignments to each series. Such assignments, which are necessarily approximate because l is not a quantum number of the system, have also been given. It should be noted that in some cases there were also signs of considerable mixing between the closed and open channels. This appeared to be particularly true for $l=0-2$ series in the $^2\Pi$ calculation. These mix strongly with the $l=2$ open channel. Indeed this mixing appears to be involved in the transfer of the broad resonance in this symmetry from being primarily p wave to d wave as R increases.

The imaginary components of the quantum defects given in tables 7 and 8 only agree approximately with those obtained directly from fitting the resonances. However, one should note that the dipole coupling between the degenerate channels can cause anomalous, even cusp-like, behaviour in the quantum defects as they cross threshold (Dubau 1978). Comparisons among tables 5–8 show that the resonance series that

Table 7. Quantum defects, (α, β), for the low-lying resonances in e^--CH^+ with $^2\Sigma$ symmetry calculated directly from above threshold. (Powers of ten given in parentheses); [a,b] indicate l values that are strongly coupled.

l/R	1.5	1.8	2.0	2.137
1	0.414 2.3 (−3)	0.411 2.2 (−3)	0.415 1.6 (−3)	0.425 1.1 (−3)
2	−0.020 6.0 (−4)	−0.022[a] 6.3 (−4)	0.027[a] 1.5 (−3)	0.038[a] 1.9 (−3)
3	−4 (−3)[a] 2.3 (−4)	0.015[a] 9.2 (−4)	−0.027[a] 7.7 (−4)	−0.031[a] 8.6 (−4)
4	1 (−3)[a] 1.7 (−4)	−3 (−3) 2.6 (−4)	−2 (−3) 3.2 (−4)	−2 (−3) 3.5 (−4)
5	−2 (−4) 7.3 (−6)	3 (−5)[b] 1.1 (−5)	2 (−4) 5.2 (−5)	4 (−4) 9.6 (−5)
6	−9 (−6) 8.7 (−8)	−3 (−5)[b] 8.1 (−6)	−1 (−5) 2.1 (−6)	−1 (−5) 1.5 (−6)

l/R	2.3	2.5	3.0
1	0.477 4.1 (−3)	0.262 1.7 (−2)	0.355 2.3 (−3)
2	0.052[a] 2.2 (−3)	0.065[a] 2.0 (−3)	0.106 2.1 (−3)
3	−0.037[a] 9.6 (−4)	−0.045[a] 1.1 (−3)	−0.065 1.5 (−3)
4	−2 (−3) 3.5 (−4)	−2 (−3) 3.4 (−4)	−3 (−3)[b] 4.0 (−4)
5	8(−4) 1.7 (−4)	1(−3) 2.2 (−4)	2(−3)[b] 3.7 (−4)
6	−1(−5) 1.3 (−6)	−1 (−5) 1.3 (−6)	−1 (−5) 1.6 (−6)

Table 8. Quantum defects, (α, β), for the low-lying resonances in e^--CH^+ with $^2\Pi$ symmetry calculated directly from above threshold. (Powers of ten given in parentheses); [a,b,c] indicate l values that are strongly coupled.

l/R	1.5	1.8	2.0	2.137
0	−0.031 3.8 (−3)	−0.029 5.7 (−3)	−0.030 3.5 (−3)	−0.032 2.4 (−3)
1	0.557 1.8 (−3)	0.550 4.2 (−2)	0.545 5.3 (−2)	0.561 7.0 (−2)
2	0.037 4.3 (−3)	0.083 9.2 (−3)	0.139 1.6 (−2)	0.212 2.1 (−2)
3	−2 (−3) 1.1 (−4)	−6 (−3)[a] 1.4 (−4)	−8 (−3)[a] 1.5 (−4)	0.015[a] 3.3 (−4)
4	2 (−3) 1.6 (−4)	5 (−3)[a] 2.6 (−4)	0.010[a] 3.4 (−4)	−0.010[a] 7.7 (−5)
5	−1 (−4) 3.5 (−6)	−8 (−5) 4.6 (−6)	−1 (−4) 4.7 (−6)	−1 (−4) 3.0 (−6)
6	−7 (−6) 5.5 (−8)	6 (−6) 4.9 (−7)	1(−5) 6.9 (−7)	2(−5) 7.3 (−7)

l/R	2.3	2.5	3.0
0	−0.036 3.7 (−3)	−0.045 9.4 (−4)	−0.073 2.1 (−4)
1	−0.092 1.6 (−3)	0.466 2.4 (−2)	0.405[a] 1.2 (−2)
2	0.407 8.6 (−2)	−0.124 0.124	0.415[a] 9.1 (−2)
3	0.030 4.4 (−3)	0.031 3.0 (−3)	0.055[b] 5.4 (−3)
4	−8 (−3) 1.2 (−3)	−0.011 5.3 (−4)	−0.016[b] 8.5 (−4)
5	8 (−5)[a] 4.7 (−5)	−9 (−5) 1.8 (−5)	1 (−4)[c] 3.4 (−5)
6	−4 (−5)[a] 2.0 (−5)	7(5) 1.6 (−5)	−1 (−4)[c] 2.5 (−5)

were not detected in the original scan all correspond to high l series with very small absolute values of μ. One would expect that for the higher l values not included in the calculation $|\mu| = 0$ can be assumed to a very good approximation.

Previous calculations of the autoionising states of CH have concentrated on the $^2\Pi$ as this symmetry has a relatively broad resonance. The quantum defects calculated here for this symmetry can be compared with the more limited calculations of Giusti-Suzor (1979). For the broadest resonance our results agree well with her values for

the '4pπ' state of $\nu = 3.442$ and 3.454 at $R = 1.5$ and 2.0 a_0 respectively, but increase faster than hers at large R, where we find considerable mixing between channels. The agreement is not so good for the d wave for which she finds α to be small (<0.02 in absolute value) and negative for all geometries.

5. Conclusions

Both bound-state and scattering calculations have been performed on the e^--CH^+ system using a number of approximations, the most sophisticated being a polarised three-coupled-state model. Complex multichannel quantum defect theory has been used to analyse the resonance structure.

With the many resonances resolved in this work there are of course many crossings between resonance curves and the CH^+ ground state. While all of these might have some significance for the dissociative recombination of CH^+, the broadest resonances must be the most important. Thus the crossing point between the broad $^2\Pi$ resonance(s) have excited most interest. Unfortunately the errors in the $CH^+(^1\Sigma^+ \rightarrow {}^3\Pi)$ excitation energy make it difficult to say definitely where this crossing occurs. However, an advantage of parametrising the problem using quantum defect theory is that it allows for corrected excitation energies to be included in a future study on the dissociative processes.

Acknowledgment

I would like to thank Professor P G Burke, Drs L A Morgan and C J Noble for helpful discussions during the course of this work, Dr P J Storey and Professor M J Seaton for their lucid explanations of quantum defect theory and the many people who made helpful comments when I reported preliminary results of this work at ICPEAC XV in Brighton.

References

Baluja K L, Burke P G and Morgan L A 1982 *Comput. Phys. Commun.* **27** 299-307
Cade P E and Huo W 1973 *At. Data Nucl. Data Tables* **12** 429
Dalgarno A 1976 *Atomic processes and Applications* ed P G Burke and B L Moiseiwitsch (Amsterdam: North-Holland) p 109
Dubau J 1978 *J. Phys. B: At. Mol. Phys.* **11** 4095-108
Elitzer M and Watson W D 1978 *Astrophys. J.* **222** L141-4
—— 1980 *Astrophys. J.* **236** 172-80
Gillan C J, Nagy O, Burke P G, Noble C J and Morgan L A 1987 *J. Phys. B: At. Mol. Phys.* **20** 4585-603
Giusti-Suzor A 1979 *PhD Thesis* L'Université de Paris-Nord
Green S, Bagus P S, Liu B, McLean A D and Yoshimine M 1971 *Phys. Rev.* A **5** 1614-8
Herzberg G and John J W C 1969 *Astrophys. J.* **158** 399-418
Lie G C, Hinze J and Liu B 1973 *J. Chem. Phys.* **59** 1872-98
Morgan L A 1984 *Comput. Phys. Commun.* **31** 419-22
Morgan L A and Burke P G 1988 *J. Phys. B: At. Mol. Opt. Phys.* submitted
Morgan L A and Noble C J 1984 *J. Phys. B: At. Mol. Phys.* **17** L369-73
Moores D L and Saraph H E 1983 *Atoms in Astrophysics* ed P G Burke *et al* (New York: Plenum) pp 173-220
Mui P M, Mitchell J B A, D'Angelo V S, De France P, McGowan J W and Froelich H 1981 *J. Phys. B: At. Mol. Phys.* **14** 1353-61
Noble C J and Nesbet R K 1984 *Comput. Phys. Commun.* **33** 399-411

Norcross D W and Seaton M J 1970 *J. Phys. B: At. Mol. Phys.* **9** 2983-3000
Ohja P C and Burke P G 1983 *J. Phys. B: At. Mol. Phys.* **16** 3513-29
Pineau des Forets G, Flower D R, Hartquist T W and Dalgarno A 1986 *Mon. Not. R. Astron. Soc.* **220** 801-24
Raseev G, Giusti-Suzor A and Lefebre-Brion H 1978 *J. Phys. B: At. Mol. Phys.* **11** 2735-47
Robb W D and Collins L A 1980 *Phys. Rev.* A **22** 2474-84
Seaton M J 1969 *J. Phys. B: At. Mol. Phys.* **2** 5-11
—— 1983 *Rep. Prog. Phys.* **46** 167-257
Schneider B I and Collins L A 1983 *Phys. Rev.* A **28** 166-8
Tennyson J 1987 *J. Phys. B: At. Mol. Phys.* **20** L375-8
Tennyson J, Burke P G and Berrington K A 1987 *Comput. Phys. Commun.* **47** 207-16
Tennyson J and Noble C J 1984 *Comput. Phys. Commun.* **32** 421-4
—— 1985 *J. Phys. B: At. Mol. Phys.* **18** 155-65
—— 1986 *J. Phys. B: At. Mol. Phys.* **19** 4025-33
Tennyson J, Noble C J and Burke P G 1986 *Int. J. Quantum Chem.* **29** 1033-42
Tennyson J, Noble C J and Salvini S 1984 *J. Phys. B: At. Mol. Phys.* **17** 905-12
van Dishoeck E F 1987 *J. Chem. Phys.* **86** 196-214